電気学会論文誌●（●●●●●●●部門誌）
IEEJ Transactions on ●●●●●●●●●●●●●●●
Vol.●● No.● pp.●-● DOI: ●.●●/ieejeiss.●●.●

Paper

Maximum Torque per Ampere and Maximum Efficiency Control Methods based on V/f control for IPM Synchronous Motor

Jun-ichi Itoh*a), Member, Yuki Nakajima*, Student Member, Goh Teck Chiang*, Student Member

(Manuscript received Jan. 00, 20XX, revised May 00, 20XX)

This paper discusses a Maximum Torque per Ampere (MTPA) and maximum efficiency control methods which are based on the Volt per Hertz (V/f) control for an Interior Permanent Magnetic Synchronous Motor (IPMSM). The V/f control is inherently a position sensorless method, therefore it is simpler than the conventional methods such as the sensorless vector control method. In addition, the MTPA and the maximum efficiency controls can be achieved by controlling the reactive power without the information of magnet pole position. The MTPA control can reduce the copper loss in IPMSM and achieve high efficiency. Furthermore, maximum efficiency control is further improving the efficiency after implemented the MTPA, which tends to reduce both the copper and iron losses. In this paper, the validity of the MTPA methods is confirmed by simulation and experimental results. From the experimental results, the output current is reduced by 76% after implemented the MTPA to control the reactive power. In addition at 0.6 p.u. torque and 1.0 p.u. motor speed, the simulation results demonstrate that the maximum efficiency control can further reduce the total losses.

Keywords : IPM synchronous motor, V/f control, maximum toque per ampere control, maximum efficiency control, reactive power

1. Introduction

IPMSM has been intensively studied due to the attractive features, high efficiency, high density and high speed rotation[(1)~(6)].

The vector control method is widely applied to drive the IPMSM. The vector control method is necessary to detect the magnet pole position by using a position sensor such as an encoder and a resolver. However, the position sensors constrain the cost in motor drive systems.

In order to remove the position sensor, several kinds of sensorless vector control methods have been studied and proposed for IPMSM[(7)~(13)]. The sensorless vector control method estimates the magnetic pole position of the IPMSM by using the motor voltage, the motor current and motor parameters. However, the calculation for the position estimation is complicated. The stabilization is difficult due to inconsistent control parameter. In addition, the error of the position estimation occurs easily when the parameters are mismatching between the controller and the motor. Especially the motor parameters will change according to the motor temperature, flux saturation and so on. As a result, it is difficult to ensure the stability of sensorless vector control.

On the other hands, open loop control which has no current regulator such as the Volt/Hertz (V/f) control methods for the PMSM have been studied[(14)~(17)]. The V/f control method does not essentially require the information of the pole position because the control algorism is implemented on γδ-flame which the δ-axis corresponding to the output voltage vector of an inverter. The control block diagram is simpler than that of the sensor less vector control. Especially, the motor parameters are not used in the control. In Ref. (14) and (15), i_d=0 control method based on V/f control for Surface Permanent Magnetic Synchronous Motor (SPMSM) has proposed. However, for the IPMSM, i_d=0 control is not effective because the reluctance torque cannot be used effectively.

On the other hand, the MTPA control methods based on the V/f control have been investigated[(16)~(17)]. The MTPA control method can be achieved by regulating the current phase to control the reactive power. Therefore, the V/f control method is effective in those applications that do not need a high response torque control such as a fan and a pump.

However, the detail of the MTPA control method is clarified only by simulations as reported in Ref. (16) and (17). In another words, the characteristics of the MTPA in IPMSM are not evaluated practically in an experiment. Furthermore, the maximum efficiency point is different from the MTPA operation on IPMSM. That is, the maximum efficiency control for IPMSM based on V/f control has not been discussed so far. Furthermore in order to apply MTPA control method based on V/f control, d and q-axis inductance values (L_d and L_q) are used. The inductance identification method based on V/f control is required to obtain the motor parameters simply.

In this paper, the characteristics of the MTPA control strategy are clarified by experimental results. Besides, the maximum efficiency control method and the inductance identification method based on V/f control are proposed.

This paper will be organized as follows; at first, the principle of the V/f control for IPMSM with a damping control is introduced. After that, the MTPA based on V/f control is described compared

a) Correspondence to: Jun-ichi Itoh. E-mail: itoh@vos.nagaokaut.ac.jp
* Nagaoka University of Technology
1603-1, Kamitomioka-machi, Nagaoka city, Niigata, Japan 940-2188

to i_d = 0 control method. Moreover, the maximum efficiency control considering iron loss is proposed.

Secondly, the identification methods for L_d and L_q based on the V/f control is proposed in chapter 4. These methods are implemented with the MTPA

Finally, the MTPA control method and the maximum efficiency control method based on V/f control method are confirmed in simulation and experimental results. The prototype uses 1.5-kW IPMSM with a two-level inverter. In addition, the inductance identification method is demonstrated in the experiment. These results indicate the validity of the proposed method.

2. High efficiency control strategy based on V/f control

2.1 V/f control based on the output voltage vector of the inverter Fig. 1 shows the relationship between γδ-frame and dq-frame. Generally, in the dq-frame of the IPMSM control, the d-axis is defined as the direction of the flux vector by the permanent magnet and the direction of the q-axis is defined as the electromotive force vector. Therefore, it is very important to identify the flux vector in the vector control. However, the V/f control method is implemented on the γδ-frame, and the δ-axis is defined as the direction of the output voltage vector of the inverter. Therefore, the δ-axis is referred as the active power component and the γ-axis is referred as the reactive power component.

The voltage equation of IPMSM based on dq-frame is given by (1).

$$\begin{bmatrix} v_d \\ v_q \end{bmatrix} = \begin{bmatrix} R_a + pL_d & -\omega_{re}L_q \\ \omega_{re}L_d & R_a + pL_q \end{bmatrix} \begin{bmatrix} i_d \\ i_q \end{bmatrix} + \begin{bmatrix} 0 \\ \omega_{re}\psi_m \end{bmatrix} \quad \text{..... (1)}$$

where $v_{d(q)}$ is the d(q)-axis voltage, $i_{d(q)}$ is the d(q)-axis current, ω_{re} is the electric angular frequency, p is the differential operator, R_a is the armature resistance value, $L_{d(q)}$ is the d(q)-axis synchronous inductance values, and ψ_m is the flux linkage of the permanent magnet. Then, the voltage equation of IPMSM based on γδ-frame is obtained by (2).

$$\begin{bmatrix} v_\gamma \\ v_\delta \end{bmatrix} = \begin{bmatrix} R_a + pL_d & -\omega_1 L_q \\ \omega_1 L_d & R_a + pL_q \end{bmatrix} \begin{bmatrix} i_\gamma \\ i_\delta \end{bmatrix} + \omega_{re}\psi_m \begin{bmatrix} \sin\theta \\ \cos\theta \end{bmatrix} \quad \text{..... (2)}$$

where $v_{\gamma(\delta)}$ is the γ(δ)-axis voltage, $i_{\gamma(\delta)}$ is the γ(δ)-axis current, and ω_1 is the rotating speed of γδ-frame. Here, the equation of the torque and the relationship between the electric angular velocity and the torque on γδ-frame is given by (3) and (4) respectively. It is noted that the viscosity resistance is ignored.

$$T = P_f \psi_m i_q = P_f \psi_m \left(i_\gamma \sin\theta + i_\delta \cos\theta \right) \quad \text{..... (3)}$$

$$p\omega_{re} = \frac{P_f \left(T - T_L \right)}{J} \quad \text{..... (4)}$$

where P_f is the pairs of poles, T is the output torque, T_L is the load torque, and J is the inertia of the motor. The gap angular θ between γδ-frame and dq-frame is given by (5).

$$p\theta = \omega_1 - \omega_{re} \quad \text{..... (5).}$$

In the steady state, the rotating speed in either γδ-frame or dq-frame is same value. However, in transient state, the gap angular between γδ-frame and dq-frame occurs due to the variation in the rotating speed. Here, the differential of θ is equaled to the difference between ω_1 and ω_{re}.

From the definition of the γδ-frame, the output voltage vector v_δ is given on δ-axis. In addition, the electromotive force $\omega_{re}\psi_m$ occurs on the q-axis. Therefore, the gap angular θ between the γ-axis and dq-frame depends on the load angular.

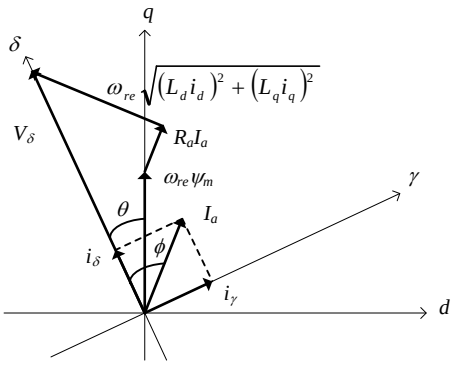

Fig. 1. Relationship between γδ-frame and dq-frame. The δ-axis is defined as the direction of the output voltage vector of the inverter, and the direction of the q-axis is defined as the electromotive force vector.

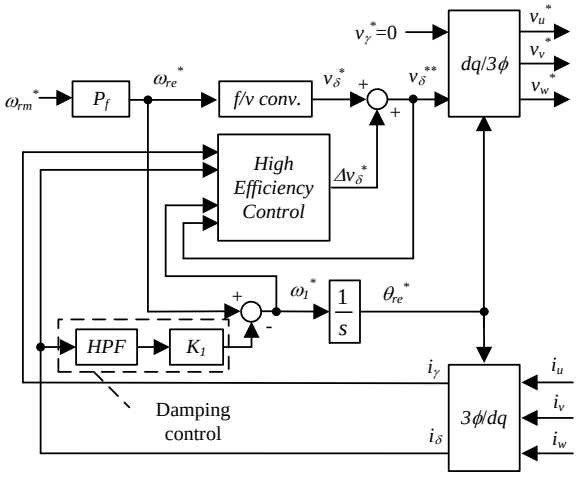

Fig. 2. V/f control method based on γδ-frame. The motor is controlled by V/f control method with damping control.

2.2 Damping control Fig. 2 shows the block diagram of the V/f control method based on γδ-frame. When motor is controlled by simple V/f control method which means an open loop control, the torque vibration is generated due to the resonance between the synchronous reactance and the moment of inertia of the IPMSM as indicated in Ref. (13).

In Ref. (13), the V/f control method based on the γδ-frame with damping control has been proposed. The torque vibration causes the vibration of the δ-axis current because the δ-axis current is an active current. In another words, the vibration component of the δ-axis current can be taken as a reference to assume the vibration component of the torque. The damping control suppresses the torque vibration with a feedback from the δ-axis current into the electric angular frequency reference value ω_{re}^* in order to cancel the load angular vibration. When the damping control is applied, the damping coefficient is a function to the feedback gain K_1, therefore, the stable operation can be achieved.

2.3 Maximum torque per ampere control based on reactive power control The reactive power on dq-frame Q_{dq} is given by (6).

$$Q_{dq} = v_q i_d - v_d i_q \quad \text{..... (6)}$$

By substituting (1) into (6) the reactive power Q_{dq} can be expressed as (7).

$$Q_{dq} = \omega_{re}\left\{L_d {i_d}^2 + L_q {i_q}^2 + \psi_m i_d\right\} \quad \text{..... (7)}$$

At first, i_d = 0 control which is often used in a SPMSM to obtain the maximum efficiency, is considered in order to compare the MTPA for IPMSM. Equation (7) can be rewritten as (8) when i_d = 0.

$$Q_{dq} = \omega_{re} L_q {i_q}^2 = \omega_{re} L_q {I_a}^2 = \omega_{re} L_q \left({i_\gamma}^2 + {i_\delta}^2\right) \quad \text{..... (8)}$$

On the other hands, the reactive power based on γδ-flame $Q_{\gamma\delta}$ is given by

$$Q_{\gamma\delta} = v_\delta i_\gamma \quad \text{..... (9)}$$

Therefore, if v_δ is regulated to confirm the reactive power which is calculated from the γδ-frame on (10), the i_d = 0 control can be achieved without the information from the dq-frame.

$$\omega_{re} L_q \left({i_\gamma}^2 + {i_\delta}^2\right) = v_\delta i_\gamma \quad \text{..... (10)}$$

Fig. 2 and Fig. 3 show the control block diagram of the i_d = 0 control method based on V/f control for IPMSM. The detail of the high efficiency block diagram in Fig. 2 is shown in Fig. 3.

On the other hand, when the IPMSM is controlled, the reluctance torque cannot be used if i_d = 0 control is applied. Therefore, the MTPA control based on V/f control for IPMSM is described as following.

Equation (7) can be rewritten as (11) by using the output current I_a and the current phase β.

$$Q_{dq} = \omega_{re}\left\{L_d {I_a}^2 \sin^2\beta + L_q {I_a}^2 \cos^2\beta - \psi_m I_a \sin\beta\right\} \quad \text{.....(11)}$$

where the equation of the β when the MTPA control[18)~(22)] is given by

$$\beta = \sin^{-1}\left(-\frac{\psi_m}{4(L_q - L_d)I_a} + \sqrt{\left(\frac{\psi_m}{4(L_q - L_d)I_a}\right)^2 + \frac{1}{2}}\right) \quad \text{.... (12).}$$

Note that the current phase β becomes zero when L_d equal to L_q i.e. it means SPMSM because 1st term equals to 2nd term. If this is defined as $I_a \sin(\beta) = X$, then the equation of the reactive power is obtained by (13).

$$Q_{dq} = \omega_{re}\left\{L_d X^2 + L_q\left({I_a}^2 - X^2\right) - \psi_m X\right\} \quad \text{..... (13)}$$

Equation (13) is the reactive power when the MTPA control is achieved. Therefore, if the $Q_{\gamma\delta}$ as shown in (9) equals to Q_{dq} as shown in (13), the MTPA control can be achieved. In another words, the satisfaction of (14) achieves the MTPA control during the V/f control.

$$\omega_{re}\left\{L_d X^2 + L_q\left({i_\gamma}^2 + {i_\delta}^2 - X^2\right) - \psi_m X\right\} = v_\delta i_\gamma \quad \text{..... (14)}$$

In order to satisfy the condition in (14), the PI controller is implemented to regulate the δ-axis voltage v_δ.

Fig. 4 shows the control block diagram of the MTPA control method based on V/f control. The control block shown in Fig. 3 is the same as the high efficiency block witch is shown in Fig. 2. In addition, the command Q_{dq} is calculated from (13) at the $Q_{dq}{}^*$ calc. block in Fig. 4. The high efficiency block conform $Q_{\gamma\delta}$ to Q_{dq}* by PI controller. The PI controller outputs the δ-axis voltage command compensation value of $\Delta v_\delta{}^*$. The $\Delta v_\delta{}^*$ compensates the δ-axis voltage command $v_\delta{}^*$ in order to accomplish (12).

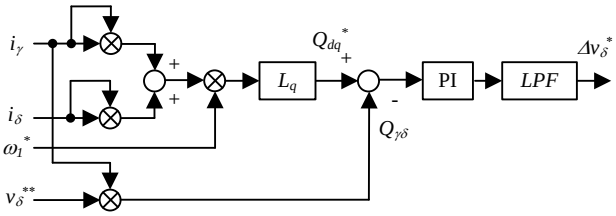

Fig. 3. Control block diagram of i_d = 0 control method based on V/f control. The $\Delta v_\delta{}^*$ compensate the δ-axis voltage command $v_\delta{}^*$ in order to accomplish (10).

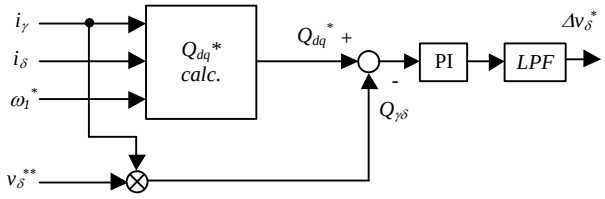

Fig. 4. MTPA control method based on the reactive power control for IPMSM. Q_{dq} command value is calculated from (13) at the Q_{dq}* calc. block

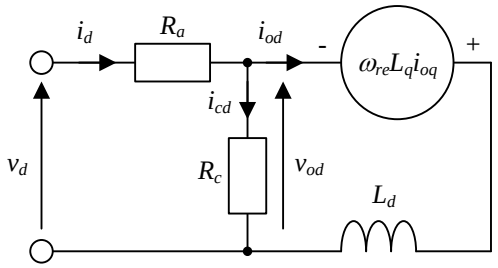

(a) d-axis

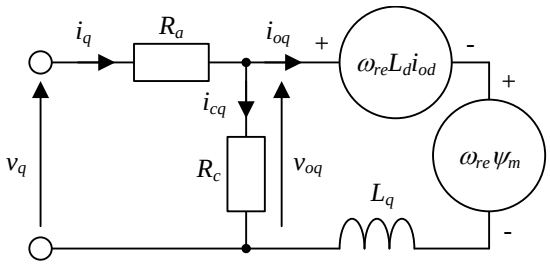

(b) q-axis

Fig. 5. Equivalent circuit considering the iron loss based on dq-frame.

2.4 Maximum efficiency control method based on V/f control The aim of MTPA control is the reduction of the copper loss of IPMSM. However, in order to improve the motor efficiency, the iron loss needs to be considered and analyzed. Then, the maximum efficiency control method based on V/f control is proposed.

Fig. 5 shows the equivalent circuit considering the iron loss based on dq-frame[23)~(24)]. Here, R_c is the equivalent iron loss resistance.

The voltage equation based on dq-frame is obtained by (15) and (16).

$$\begin{bmatrix} v_d \\ v_q \end{bmatrix} = R_a \begin{bmatrix} i_{od} \\ i_{oq} \end{bmatrix} + \left(1 + \frac{R_a}{R_c}\right)\begin{bmatrix} v_{od} \\ v_{oq} \end{bmatrix} + p\begin{bmatrix} L_d & 0 \\ 0 & L_q \end{bmatrix}\begin{bmatrix} i_{od} \\ i_{oq} \end{bmatrix} \quad \text{..... (15)}$$

$$\begin{bmatrix} v_{od} \\ v_{oq} \end{bmatrix} = \begin{bmatrix} 0 & -\omega L_q \\ \omega L_d & 0 \end{bmatrix} \begin{bmatrix} i_{od} \\ i_{oq} \end{bmatrix} + \begin{bmatrix} 0 \\ \omega \Psi_a \end{bmatrix} \quad \text{..... (16)}$$

Here, i_{od} and i_{oq} are given by (17) and (18).

$$i_{od} = i_d - i_{cd} = i_d + \frac{\omega L_q i_{oq}}{R_c} \quad \text{..... (17)}$$

$$i_{oq} = i_q - i_{cq} = i_q - \frac{\omega\left(\Psi_a + L_d i_{od}\right)}{R_c} \quad \text{..... (18)}$$

In addition, the iron loss W_i is given by (19)

$$W_i = \frac{V_o^{\,2}}{R_c} = \frac{\left(\omega_{re} L_q i_{oq}\right)^2 + \left(\omega_{re} L_d i_{od} + \omega_{re}\psi_m\right)^2}{R_c} \quad \text{..... (19)}$$

Therefore, in order to achieve the maximum efficiency control, considering of not only the copper loss but also the iron loss is important.

The reactive power reference value of maximum efficiency control method is obtained from (20).

$$Q_{dq} = Q_{dqref\_cmp} + \omega_{re}\left\{L_d X^2 + L_q\left(I_a^{\,2} - X^2\right) - \psi_m X\right\} \text{..... (20)}$$

From the MTPA control based on V/f control, it is confirmed that the current phase can be controlled indirectly by control of the reactive power. Therefore, Q_{dqref} is varied by the reactive power reference compensation value Q_{dqref_cmp} and the current phase is regulated. As the result, the maximum efficiency point can be found.

3. Identification methods for L_d and L_q based on the V/f control

3.1 q-axis inductance identification method based on MTPA control method The MTPA control method based on V/f control requires the information of motor parameters. Therefore, if the motor parameter is different from the actual value, the $Q_{dq}^{\,*}$ might not become an appropriate value to minimize the I_a. Therefore, the estimation of reactance of the IPMSM is required. Here, by using $i_d = 0$ control method based on the V/f control, the q-axis inductance value L_q can be identified.

Here, (8) is transformed into (21), when L_{q_est} is the estimation value of L_q.

$$Q_{dq}^{\,*} = \omega_{re} L_{q\_est}\left(i_\gamma + i_\delta\right)^2 \quad \text{..... (21)}$$

As following, when L_{q_est} is equaled to L_q, $i_d = 0$ control can be achieved. Therefore, by varying the L_{q_est} and observing the d-axis current, then L_q is possible to estimate.

However, during the V/f control, d-axis current cannot be observed directly because the magnet pole position is not used. As the result, $i_d = 0$ can be determined by (22).

$$v_\delta^{\,2} = \left(\omega_{re}\psi_m + R_a I_a\right)^2 + \left(\omega_{re} L_{q\_est} I_a\right)^2 \quad \text{..... (22)}$$

Equation (22) is valid only when $i_d = 0$ because the vector directions of $\omega_{re}\psi_m$ and $R_a I_a$ become the same when $i_d = 0$ (shown in Fig. 6). Then, L_{q_est} can be assumed to be equaled to L_q. That is, the i_d=0 point is found out by comparison between right term and left term of (22) without rotor position information. Note that the proposed estimation method for L_q does not use L_d. Therefore, L_q is estimated independently.

3.2 d-axis inductance identification method based on MTPA control method Using MTPA control method based on V/f control, the d-axis inductance value L_d can be identified.

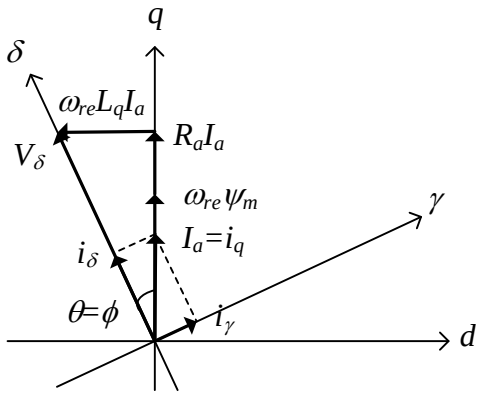

Fig. 6. Vector diagram of the IPMSM driven by V/f control when i_d = 0 control. The vector directions of $\omega_{re}\psi_m$ and $R_a I_a$ become the same when $i_d = 0$

First, (13) is transformed into (23), when L_{d_est} is the estimation value of L_d.

$$Q_{dq}^{\,*} = \omega_{re}\left\{L_{d\_est} X^2 + L_q\left(I_a^{\,2} - X^2\right) - \psi_m X\right\} \text{..... (23)}$$

As following, when L_{q_est} is equaled to L_q, the output current I_a becomes its minimum. Therefore, by varying the L_{q_est} and observing the I_a, and then the L_d can be estimated.

However, if L_q is different from the actual value, I_a might become smaller when L_{d_est} is not equaled to L_d. Therefore, L_q should be estimated by using the proposed L_q identification method that has been discussed in this chapter.

4. Simulation results

4.1 Maximum efficiency control method based on V/f control Fig. 7 shows the simulation result when Q_{dqref_cmp} varies and R_c is assumed to be 300 Ω. The minimum point of the total loss Wc + Wi is Q_{dqref_cmp} = 0 p.u., when ω_{rm} is 0 p.u.. On the other hand, the minimum point of the total loss is Q_{dqref_cmp} = -0.4 p.u. when ω_{rm} is 1.0 p.u. From the results, it is confirmed that the current phase varies when the total loss becomes minimum since the rotating speed of the motor is changed because the iron loss varies

Fig. 8 shows the values of Q_{dqref_cmp} that can achieve the lowest losses subject to the motor speed. From Fig. 8, the equation of Q_{dqref_cmp} can be expressed by (24).

$$Q_{dqref\_cmp} = A\omega_{rm}^{\,2} + B\omega_{rm} \quad \text{..... (24)}$$

Here, in this IPMSM, A and B are -0.547 and 0.141 respectively from the curve in Fig. 8.

Fig. 9 shows the amplitude of the total loss when the reactive power reference value is varied by adding the error Q_{dqref_vary} as expressed in (25).

$$\begin{aligned} Q_{dq} &= Q_{dqref\_vary} + Q_{dqref\_cmp} \\ &\quad + \omega_{re}\left\{L_d X^2 + L_q\left(I_a^{\,2} - X^2\right) - \psi_m X\right\} \end{aligned} \quad \text{..... (25)}$$

Here, Q_{dqref_cmp} from (24) is substituted into (25) and Q_{dqref} will be compensated depending on ω_{rm}. When Q_{dqref_vary} is zero, it is confirmed that total loss can be reach its minimum.

4.2 d and q-axis inductance identification method based on MTPA control method Fig. 10 shows the simulation result of L_q identification method. Here, the horizontal axis is the ratio between L_{q_est} and L_q, and the vertical axis is the difference between right and left sides of (22). The simulation conditions are

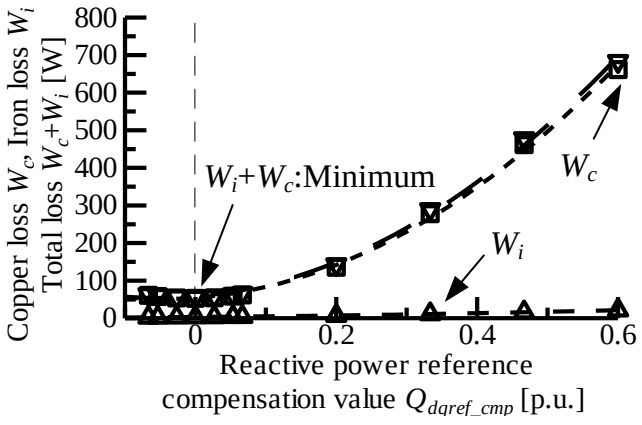

(a) ω_{rm} = 0p.u.

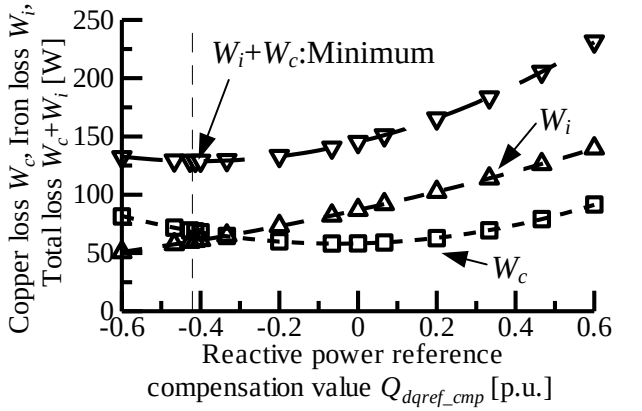

(b) ω_{rm} = 1.0p.u.

Fig.7. Relationship between Q_{dqref_cmp} and the total loss (Load torques are 1.0 p.u.).

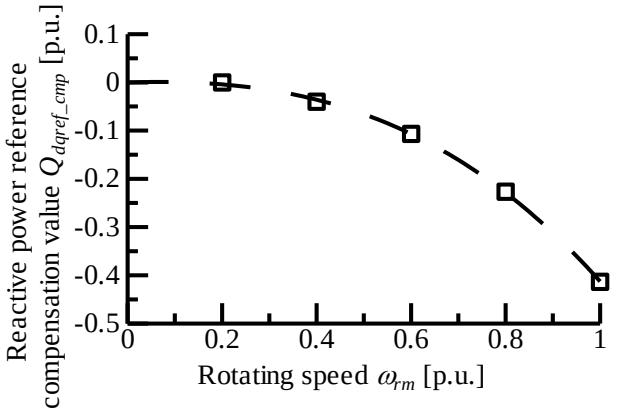

Fig. 8. Relationship between ω_{rm} and Q_{dqref_cmp} when the total loss minimum (Load torques are 1.0 p.u.).

follows; the rotating speed command value is 1.0 p.u. and the load torque is 1.0 p.u. When the difference between left and right sides of (22) is equaled to 0, it is confirmed that i_d = 0 and L_{q_est} is equaled to L_q. As the result, it is confirmed that this method can estimate the L_q.

Fig. 11 shows the simulation result of L_d identification method. The horizontal axis is the ratio between L_{q_est} and L_q, and the vertical axis is the output current value I_a. The simulation conditions are follows; the rotating speed command value is 1.0 p.u. and the load torque is 1.0 p.u. When I_a becomes its minimum,

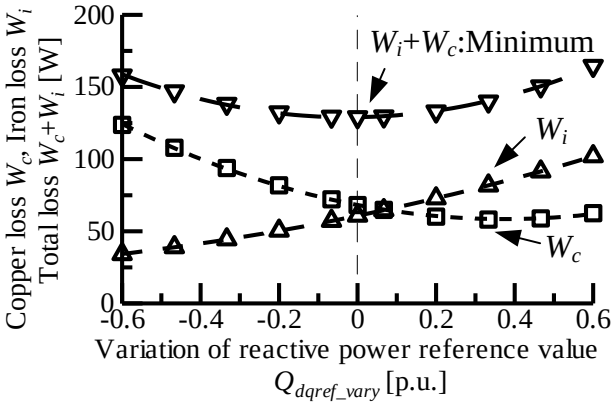

Fig. 9. Relationship between Q_{dqref_vary} and the total loss with Maximum Efficiency control (Load torques are 1.0 p.u. and rotating speeds are 1.0 p.u.)

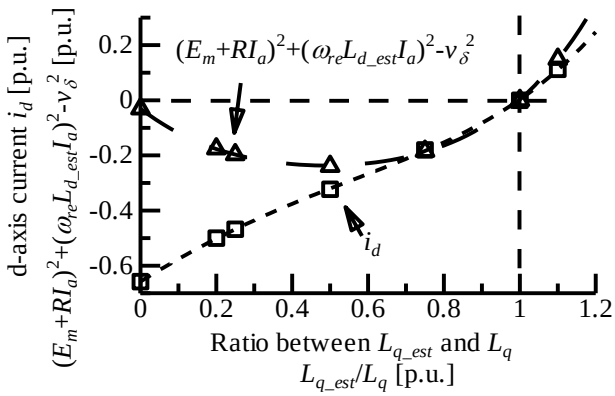

Fig. 10. Relationship between L_{q_est}/L_q, i_d and the discriminant (Load torques are 1.0 p.u. and rotating speeds are 1.0 p.u.).

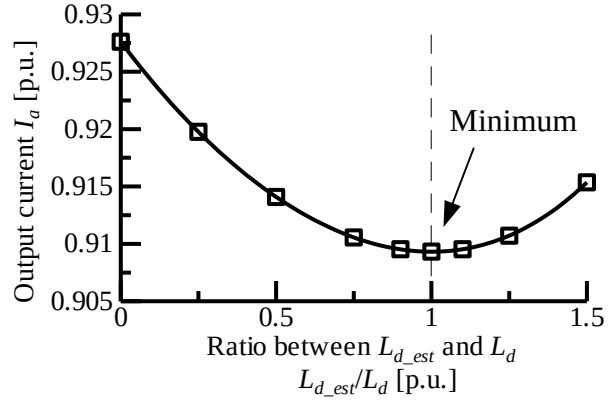

Fig. 11. Relationship between L_{d_est}/L_d and I_a (Load torques are 1.0 p.u. and rotating speeds are 1.0 p.u.).

the result can confirm that L_{d_est} is equaled to L_d. As the result, it is confirmed that this method can estimate the L_d.

5. Experimental results

5.1 Maximum torque per ampere control method based on V/f control Fig. 12 show the schematic of the experimental system. The IPMSM is driven by a two-level

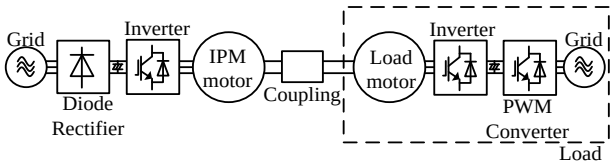

Fig. 12. Schematic of the experimental system.

Table 1. Motor parameter using the experiment.

Motor Power	1.5kW
Rated Current	6.1A$_{rms}$
Rated Speed	1800rpm
Number of Poles	6poles
Winding Resistance	0.783Ω
d-axis Inductance	11.5mH
q-axis Inductance	23.0mH
Interlinkage magnetic flux	0.246V･s/rad

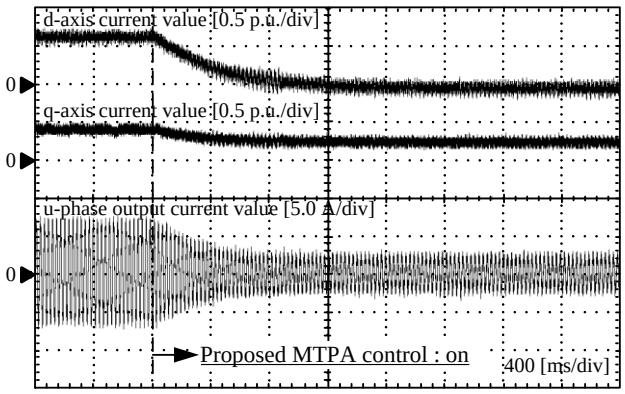

Fig. 13. Variation of the dq-frame and u-phase current by the MTPA control method based on V/f control (Load torque is 0.2p.u. and rotating speed is 0.4p.u.). The output current can be reduced by 68 % (from 0.72 p.u. to 0.23 p.u.) after applying the MTPA control method.

inverter and the switching frequency is 10 kHz. In addition, the load motor is used as load machine to supply a constant torque. In this experiment, in order to confirm the effectiveness of the MTPA control method based on V/f control, the information of magnet pole position is obtained from a Hall Effect sensor. However, the information of magnet pole position is not used in the actual motor drive system.

Table 1 shows the motor parameters that are used in the experiment. The IPMSM has a saliency ratio of 2.0.

Fig. 13 shows the experimental results of the IPMSM drive operation using the two-level inverter with the MTPA control method based on the V/f control method. The experimental conditions are follow; the rotating speed command value is 0.4 p.u. and the load torque is 0.2 p.u.. From Fig. 4, the output current can be reduced by 68 % (from 0.72 p.u. to 0.23 p.u.) after applying the MTPA control method. If the MTPA control is disabled, the reluctance torque cannot reach its maximum and the output current becomes large. On the other hand, if the MTPA control is enabled, the reluctance torque can reach its maximum and the output current becomes its minimum.

Fig. 14 shows the amplitude of the output current when the reactive power is varied by adding the error Q_{dqref_vary} as (26).

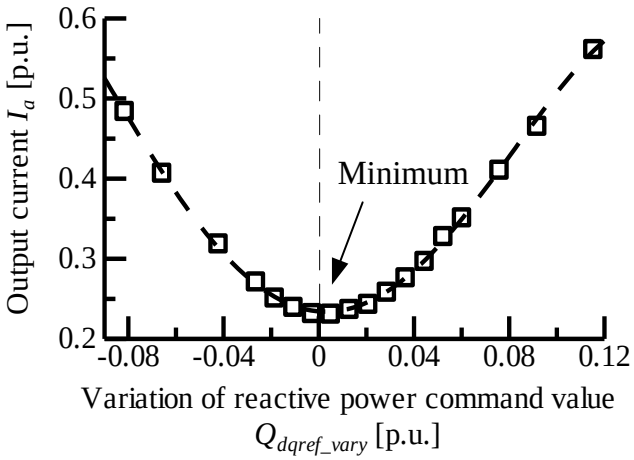

Fig. 14. Relationship between Q_{dqref_vary} and I_a with MTPA control method (Load torques are 0.2p.u. and rotating speeds are 0.2p.u.). The amplitude of the output current becomes minimum at 0.23 p.u. when the reactive power command value is equivalent to the theoretical value.

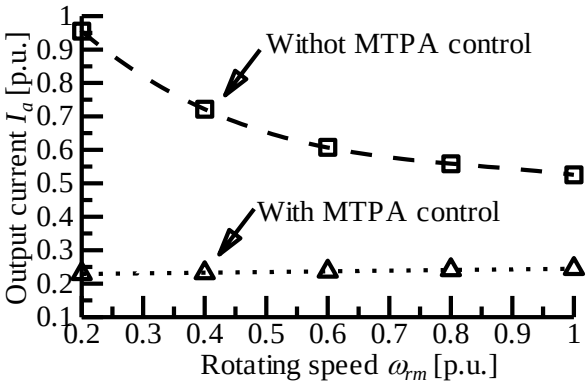

Fig. 15. Variation of the output current with/without MTPA control method when rotating speed is changed (Load torques are 0.2p.u.). Even if the load condition is varying, the proposed method can reduce the output current.

$$Q_{dq}^{*} = Q_{dqref\_vary} + \omega_{re}\left\{L_d X^2 + L_q\left(I_a^{\,2} - X^2\right) - \psi_m X\right\} \quad ..(26).$$

In Fig. 14, the horizontal axis shows the difference between the reactive power command value and the theoretical value Q_{dqref}. It is confirmed that the amplitude of the output current becomes minimum at 0.23 p.u of the rated current. when the reactive power command value is equivalent to the theoretical value. It means that the reactive power command from (13) can minimize the output current at the constant load torque. As a result, the effectiveness of the MTPA method can be observed.

Fig. 15 shows the amplitude of output current when the load condition varies. Even if the load condition varies, the MTPA method can reduce the output current. In addition, the output current can be reduced by 76 % (from 0.96 p.u. to 0.23 p.u.).

5.2 Maximum efficiency control method based on V/f control Fig. 16 shows the experimental results to confirm the operation of the maximum efficiency control. The schematic of the experimental system is shown in Fig. 12. The experimental conditions are follow; the rotating speed command value is 1.0 p.u.

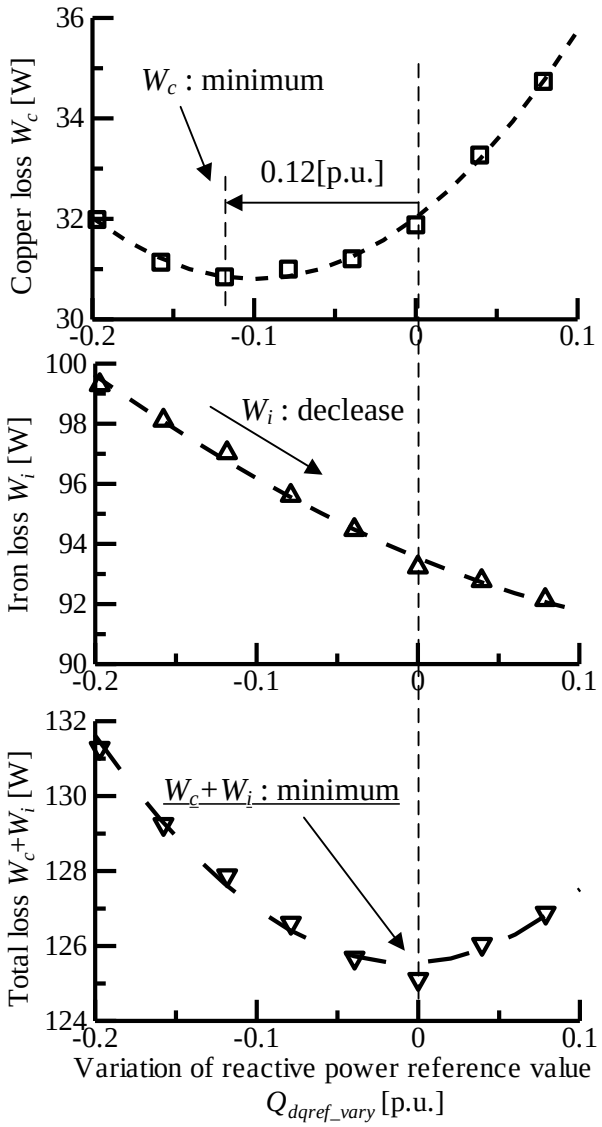

Fig. 16. The relationships between the Q_{dqref_vary} and the copper loss, iron loss, and total loss with maximum efficiency control (Load torques are 0.6 p.u. and rotating speeds are 1.0 p.u.)

and the load torque is 0.6 p.u.. Here, Q_{dqref_cmp} as expressed in (25) is set at 0.12 p.u.

The horizontal axis is the error Q_{dqref_vary} as expressed in (25), and the copper loss, iron loss and total loss are varied by the Q_{dqref_vary}. When Q_{dqref_vary} is zero, the total loss can reach its minimum that is 125.1 W. As the result, the maximum efficiency control can be achieved. Furthermore, when Q_{dqref_vary} is -0.12 p.u., the copper loss reaches the minimum 30.8 W whereas the total loss is not the smallest because iron loss increases. From the result, the maximum efficiency control demonstrated that the total losses are further reduced by 2.8 W compared to the MTPA control based on V/f control. Therefore, it is confirmed that the maximum efficiency control can achieve higher efficiency than the MTPA control.

5.3 d and q-axis inductance identification method based on MTPA control method Fig. 17 shows the experimental result of L_q identification method. Here, the horizontal axis is the ratio between L_{q_est} and L_q, and the vertical

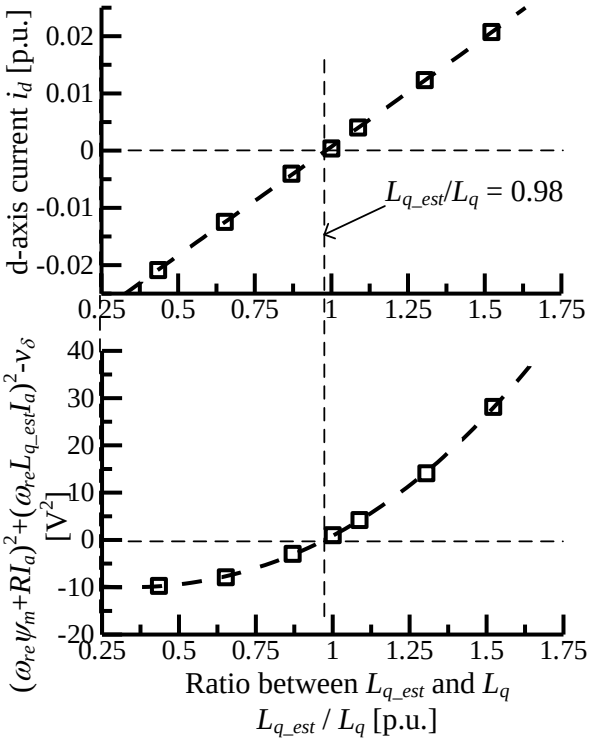

Fig. 17. Variation of the output current with/without MTPA control method when rotating speed is changed (Load torques are 0.2p.u.).

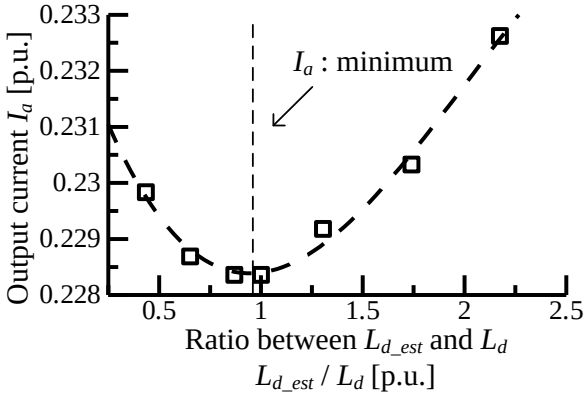

Fig. 18. Variation of the output current with/without MTPA control method when rotating speed is changed (Load torques are 0.2p.u.).

axis is the d-axis current and also the difference between left and right sides of (22). The experimental conditions are follows; the rotating speed command value is 0.2 p.u. and the load torque is 0.2 p.u. When the difference between the left and right sides of (22) is equaled to 0, it is confirmed that i_d = 0 and L_{q_est} is equaled to 0.98 L_q (22.6 mH). As the result, it is confirmed that this method can achieve to estimate the L_q.

Fig. 18 shows the experimental result of L_d identification method. The horizontal axis is the ratio between L_{d_est} and L_d, and the vertical axis is the output current value I_a. The experimental conditions are follows; the rotating speed command value is 0.4 p.u. and the load torque is 0.2 p.u. When I_a becomes its minimum, the result can confirm that L_{d_est} is equaled to 0.95 L_d (10.9 mH).

As the result, it is confirmed that this method can achieve to estimate the L_d.

6. Conclusion

This paper discussed and evaluated a maximum torque per ampere and maximum efficiency control methods based on V/f control by simulation and experimental results.

The MTPA control method is based on the control of reactive power and as a result the information of the magnet pole position is not necessary. From the experimental results, it can confirm that the output current can be reduced by 76 %.

Furthermore, the validity of the maximum efficiency control method based on V/f control was confirmed in simulation and experimental results. The proposed method can minimize the total losses. From the result, the maximum efficiency control demonstrated that the total losses are further reduced by 2.8 W compared to the MTPA control based on V/f control.

In addition, the identification method of the L_d and L_q with the MTPA control method was proposed. From the experimental results, L_{q_est} is equaled to 0.98 L_q (22.6 mH), L_{d_est} is equaled to 0.95 L_d (10.9 mH). That is, the estimation error is within 5% of the nominal value.

These results are shown to be benefit in the construction of high efficiency sensorless IPMSM drive system that uses a V/f control.

References

(1) K. Hiramoto, S. Morimoto , Y. Takeda, "Torque ripple improvement for synchronous reluctance motor using an asymmetric flux barrier arrangement", IEEE Transactions on Industry Applications, vol. 40, no. 4, pp. 1076-1082, 2004.

(2) C.E. Nino-Baron, E.G. Strangas, "Iron and Magnet Losses and Torque Calculation of Interior Permanent Magnet Synchronous Machines Using Magnetic Equivalent Circuit", IEEE Transactions on Magnetics, vol. 46, no. 12, pp. 4073-4080, 2010.

(3) Yu-Seok Jeong, Yong-Jae Kim, Sang-Yong Jung, "Novel Analysis and Design Methodology of Interior Permanent-Magnet Synchronous Motor Using Newly Adopted Synthetic Flux Linkage", IEEE Transactions on Industrial Electronics, vol. 58, no. 9, pp. 3806-3814, 2011.

(4) P. Sergeant, F. De Belie, J. Melkebeek, "Rotor Geometry Design of Interior PMSMs With and Without Flux Barriers for More Accurate Sensorless Control", IEEE Transactions on Industrial Electronic, vol. 59, no. 6, pp. 2457-2465 , 2012.

(5) 5] Roberto H. Moncada, Juan A. Tapia, Thomas M. Jahns, "Analysis of Negative-Saliency Permanent-Magnet Machines", IEEE Transactions on Industrial Electronics, vol. 57, no. 1, pp. 122-127, 2010

(6) I. Petrov, J. Pyrhonen, "Performance of low cost permanent magnet material in PM synchronous machines", IEEE Transactions on Industrial Electronics, vol. PP, no. 99, pp. 1, 2012

(7) M. J. Corley, and R. D. Lorenz, "Rotor Position and Velocity Estimation for a Salient-Pole Permanent Magnet Synchronous Machine at Standstill and High Speeds", IEEE Transactions on Industry Applications, vol. 34, no. 4, pp. 784-789, 1998.

(8) S. Morimoto, K. Kawamoto, M. Sanada, Y. Takeda, "Sensorless control strategy for salient-pole PMSM based on extended EMF in rotating reference frame", IEEE Transactions on Industry Applications, vol. 38, no. 4, pp. 1054-1061, 2002.

(9) Zhiqian Chen, M. Tomita, S. Doki, S. Okuma, "An extended electromotive force model for sensorless control of interior permanent-magnet synchronous motors", IEEE Transactions on Industrial Electronics, vol. 50, no. 2, pp. 288-295, 2003.

(10) S. Ogasawara, H. Akagi, "Implementation and position control performance of a position-sensorless IPM motor drive system based on magnetic saliency", IEEE Transactions on Industry Applications, vol. 34, no. 4, pp. 806-812, 1998.

(11) T. Noguchi, S. Kohno, "Mechanical-Sensorless Permanent-Magnet Motor Drive Using Relative Phase Information of Harmonic Currents Caused by Frequency-Modulated Three-Phase PWM Carriers", IEEE Transactions on Industry Applications, vol. 39, no. 4, pp. 1085-1092, 2003.

(12) M. Hasegawa, S. Yoshioka, K. Matsui, "Position Sensorless Control of Interior Permanent Magnet Synchronous Motors Using Unknown Input Observer for High-Speed Drives", IEEE Transactions on Industry Applications, vol. 45, no. 3, pp. 938-946, 2009.

(13) R. Leidhold, "Position Sensorless Control of PM Synchronous Motors Based on Zero-Sequence Carrier Injection", IEEE Transactions on Industrial Electronics, vol. 58, no. 12, pp. 5371-5379, 2011.

(14) J. Itoh , N. Nomura , H. Ohsawa, "A Comparison between V/f Control and Position-Sensorless Vector Control for the Permanent Magnet Synchronous Motor", Proc. of the Power Conversion Conference PCC Osaka 2002, Vol. 3, pp. 1310-1315, 2002.

(15) JP Patent, P2000-232800A, 2000.

(16) JP Patent, P2000-262089A, 2000

(17) Shinn-Ming Sue, Tsai-Wang Hung, Jenn-Horng Liaw, Yen-Fang Li, Chen-Yu Sun, " A new MTPA control strategy for sensorless V/f controlled PMSM drives", 6th IEEE Conference on Industrial Electronics and Applications 2011, pp. 1840-1844, 2011.

(18) THOMAS M. JAHNS, GERALD B. KLIMAN, THAMAS W. NEUMANN, " Interior Permanent-Magnet Synchronous Motors for Adjustable-Speed Drives", IEEE Transactions on Industry Applications, vol. IA-22, no. 4, pp. 738-747, 1986.

(19) S. Morimoto, Y. Takeda, K. Hatanaka, Y.Tong, T. Hirasa, "Design and control system of inverter-driven permanent magnet synchronous motors for high torque operation", IEEE Transactions on Industry Applications, vol. 29, no. 6, pp. 1150-1155, 1993.

(20) Shinn-Ming Sue, Ching-Tsai Pan, "Voltage-Constraint-Tracking-Based Field-Weakening Control of IPM Synchronous Motor Drives", IEEE Transactions on Industrial Electronics, vol. 55, no. 1, pp. 340-347, 2008

(21) Bing Cheng, T.R. Tesch, "Torque Feedforward Control Technique for Permanent-Magnet Synchronous Motors", IEEE Transactions on Industrial Electronics, vol. 57, no. 3, pp. 969-974, 2010

(22) G. Foo, M.F. Rahman, "Sensorless Sliding-Mode MTPA Control of an IPM Synchronous Motor Drive Using a Sliding-Mode Observer and HF Signal Injection", IEEE Transactions on Industrial Electronics, vol. 57, no. 4, pp. 1270-1278, 2010

(23) Roy S. Colby, Donald W. Novotny, "Efficient Operation of Surface-Mounted PM Synchronous Motors", IEEE Transactions on Industry Applications, vol. IA-23, no. 6, pp. 1048-1054, 1987

(24) S. Morimoto, Y. Tong, Y. Takeda T. Hirasa, " Loss minimization control of permanent magnet synchronous motor drives", IEEE Transactions on Industrial Electronics, vol. 41, no. 5, pp. 511-517, 1994.

Jun-ichi Itoh

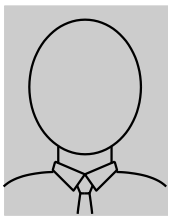

(Member) received his M.S. and PhD degrees in electrical and electronic systems engineering from Nagaoka University of Technology, Nagaoka, Japan in 1996 and 2000, respectively. From 1996 to 2004, he was with Fuji Electric Corporate Research and Development Ltd., Tokyo, Japan. Since 2004, he has been with Nagaoka University of Technology as an associate professor. He received the IEEJ Academic Promotion Award (IEEJ Technical Development Award) in 2007. His research interests include matrix converters, DC/DC converters, power factor correction techniques and motor drives. He is a member of the Institute of Electrical Engineers of Japan.

Yuki Nakajima

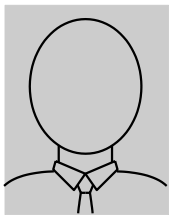

(Student Member) received his B.S. degrees in electrical, electronics and information engineering from Nagaoka University of Technology, Nagaoka, Japan in 2011. Since 2011, he has been with Nagaoka University of Technology as a M.S. degree student in electrical, electronics and information engineering. His research interests include motor drive system for Interior Permanent Magnetic Synchronous Motor. He is a student member of the Institute of Electrical Engineers of Japan.

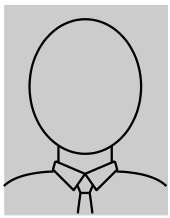

Goh Teck Chiang (Student member) received his B.S. degree in electrical and electronic engineering from Queensland University of Technology, Brisbane, Australia in 2004. Then, he received his M.S. and Ph.D. degrees in electrical and electronic systems engineering from Nagaoka University of Technology, Nagaoka, Japan in 2009 and 2012, respectively. He is currently working as a researcher in Nagaoka University of Technology. His research interests include indirect matrix converters, PWM and motor drive.